THERMAL PERFORMANCE OF A NAM-JU NANOSTRUCTURED COPPER OSCILLATING HEAT PIPE

A Thesis

presented to

the Faculty of the Graduate School

at the University of Missouri-Columbia

In Partial Fulfillment

of the Requirements for the Degree

Master of Science

---

by

STEFAN STOVER

Dr. Robert Winholtz, Thesis Advisor

December 2018

The undersigned, appointed by the dean of the Graduate School, have examined the thesis entitled

THERMAL PERFORMANCE OF A NAM-JU NANOSTRUCTURED COPPER OSCILLATING HEAT PIPE

presented by Stefan Stover,

a candidate for the degree of master of science,

and hereby certify that, in their opinion, it is worthy of acceptance.

_____

Professor Robert Winholtz

_____

Professor Hongbin Ma

_____

Professor Helmut Kaiser

Dedication

To my parents, Hans and Julie, who taught me to work hard and pursue my passions, thank you for your endless support. To my sisters, Lauren and Anna, for always bringing a smile to my face, through the good times and bad.

Finally, to my wife, Emilee. Your love and support throughout this process is immeasurable, as is my love for you. Thank you for all you have done, and all you continue to do.

Acknowledgements

I would like to express my gratitude to my advisor Dr. Robert (Andy) Winholtz, you have been an excellent mentor throughout this process. I would like to thank you for taking me on as a graduate student and providing me with the resources necessary to complete this project. I would also like to thank my committee members Dr. Hongbin Ma and Dr. Helmut Kaiser for serving in this capacity, I appreciate all comments or suggestions you may have. Thanks are due to the University of Missouri physics department and James Torres for providing the heat pipe assembly and guiding me through the Nam-Ju oxidation process necessary for this project. I'm grateful for your advice and insight regarding the oxidation procedure.

Table of Contents

Nomenclature

- Nam-Ju oxide = Copper (II) oxide created following procedure outlined by Nam and Ju
- COM = Mass of the fully charged (filled with water) oscillating heat pipe
- EOM = Mass of the fully evacuated (~0.15 Torr) oscillating heat pipe
- TOM = Target mass of the charged oscillating heat pipe
- OOM = Observed mass of the charged oscillating heat pipe
- WM = Mass of the water fully filling the oscillating heat pipe
- DWM = Desired mass of the water inside the oscillating heat pipe
- FP = Fill percent of water-by-mass desired in the oscillating heat pipe (50%, 65%, etc)
- OP = Observed fill percent of water-by-mass in the oscillating heat pipe

Acronyms

- OHP = Oscillating Heat Pipe
- HCl = Hydrochloric Acid
- DI = Deionized Water
- HPLC = High Performance Liquid Chromatography

List of Figures

List of Tables

Abstract

As electronic devices increase in performance and decrease in size, more efficient thermal management systems are necessary to combat high heat fluxes. Copper heat pipes, and oscillating heat pipes are devices commonly used in the electronics industry to remove high heat fluxes, safeguarding sensitive electronic components from thermal damage. The surface application of cupric oxide nanostructures to the interior heat pipe channel leads to a reduction of temperatures in the evaporator region of the oscillating heat pipe assembly by as much as 59.1%. The application of cupric oxide nanostructures to the oscillating heat pipe surfaces provides a simple and effective way to further reduce temperature differences between the evaporator and condenser regions of a copper oscillating heat pipe.

1 Introduction

1.1 Background

Throughout recent decades, electronic devices continue to shrink in size, increase in performance, and generate more heat. Oscillating heat pipes (OHPs), devices used to transfer and remove heat, are becoming widely used in the electronic and other industries to protect sensitive equipment from thermal damage. Shown in Figure 1.1, an OHP consists of an elongated pipe shaped in a sealed loop, inside which a bi-phase working fluid undergoes vaporization and condensation, allowing for the movement of heat from an evaporator region to a condenser region, without the use of an internal wicking structure [1, 2]. The interior of the OHP must be small enough to allow significant capillary force to form liquid slugs and vapor bubbles of the working fluid, separating the working fluid into distinct and impenetrable regions inside the OHP [3]. Vaporization, condensation, and thermal expansion of the working fluid creates pressure that causes growth and shrinkage of bubbles of working fluid vapor and slugs of working fluid liquid [4, 5]. Growth and shrinkage of slugs and bubbles occur in a cyclic manner, pushing and pulling on both phases of the working fluid, creating an oscillating movement of the working fluid inside the channels of the OHP [6]. The oscillation of slugs and bubbles, as well as phase change heat transfer, allows for the OHP to operate as a passive cooling system that can be manufactured out of many materials, use various working fluids, have very thin structures, and excel at transferring heat [7].

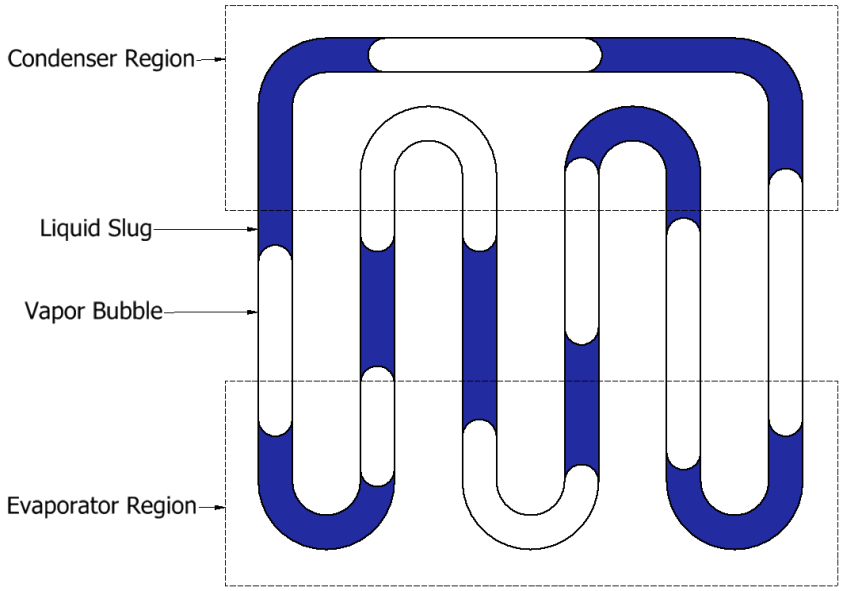

Figure 1.1. Diagram of a closed loop OHP with multiple turns, blue sections represent liquid slugs, white sections represent vapor bubbles.

Studies on improving performance of OHPs have often revolved around hydrophilic, hydrophobic, and nanostructured surfaces, primarily on copper OHPs. Increasing the surface wettability of copper can reduce water droplet angle from ~60° to as low as 0-12.9° and increase displacement of liquid slugs inside the OHP by as much as 60% [8]. Fill ratio of working fluid inside an OHP also influences thermal performance. A previous study by F. Zhang shows that hierarchical cupric oxide (CuO) surface growth on interior sections of OHPs provides high wettability of the affected surfaces, influencing the displacement of working fluid inside the OHP and affecting the ability of the OHP to reduce heat fluxes [9]. However, the hierarchical CuO growth on the OHP surfaces was difficult to accomplish in a uniform manner, leading to patches of minimal oxidation [10]. In a 2011 article, Y. Nam and Y. S. Ju discuss a method of uniform cupric oxide deposition, creating a thin layer of copper (II) oxide by immersing copper plate in a liquid solution of sodium chlorite, sodium hydroxide, and sodium phosphate dodecahydrate. This copper (II) oxide, referred to as the Nam-Ju oxide or nano oxide, is created

in a uniform layer over all copper surfaces exposed to the solution, and reduces water droplet contact angle to ~20° [11].

1.2 Experiment Purpose

The addition of the Nam-Ju copper (II) oxide to the interior surfaces of an OHP may increase the performance of the OHP by increasing heat transfer. To accurately compare OHP performance in its natural oxide and Nam-Ju oxide state, a single two-piece flat plate copper OHP is used for testing. Baseline testing is performed by evacuating, charging, and testing the OHP with its natural oxide surface conditions over a wide range of thermal inputs. Temperature readings from the evaporator and condenser regions of the OHP are recorded throughout the range of heat input. Secondary testing involves the removal of the natural copper oxide from the interior surfaces of the OHP and applying the Nam-Ju oxide to all surfaces of the OHP. Evacuation, charging, and testing procedures for the Nam-Ju oxidized OHP remain identical to the baseline testing, allowing for accurate comparisons in performance. Temperature difference between evaporator and condenser regions of the OHP are used to determine thermal performance, with lower temperature difference suggesting improved heat spreading.

2 Experimental

2.1 OHP Assembly

This study focuses on utilizing OHPs for electronic cooling purposes, as such the OHP is designed to resemble traditional closed loop flat plate OHPs, but with separate halves to allow for disassembly, oxidation of inner channels, and reassembly. The two halves of the OHP are machined from copper, the bottom half, visible in Figure 2.1, being 2.5 mm thick with an

internal channel in a closed loop, a fill pipe connected to the inner channels, a rectangular groove along the outer edge, and 34 holes around the rectangular groove. The upper half is a flat plate of 1.0 mm thickness with 34 holes around the outer edge.

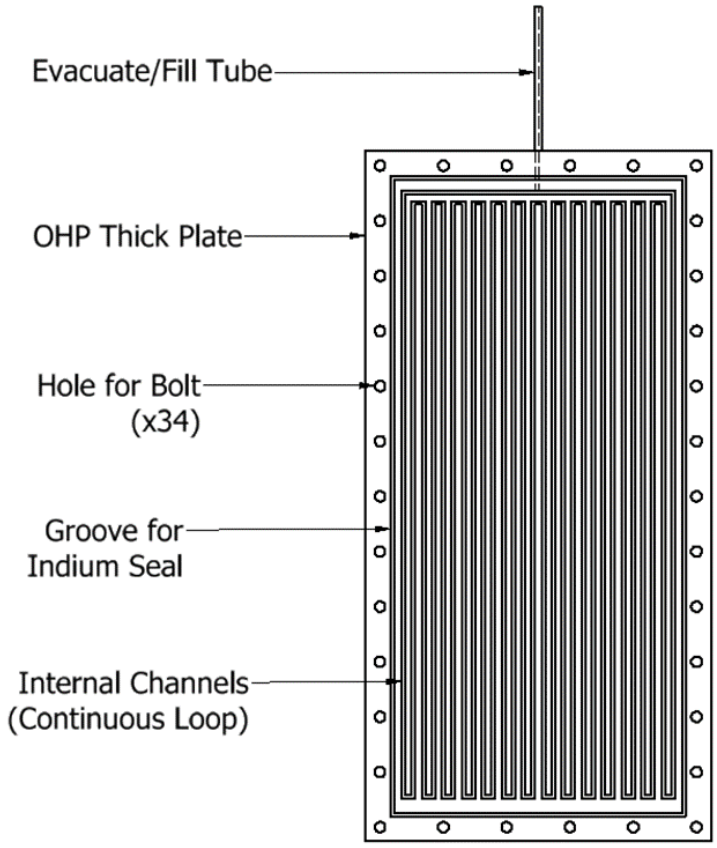

Figure 2.1. Diagram of OHP thick plate (bottom half).

Both halves of the OHP were washed in a 2.0 M solution of hydrochloric acid (HCL) to remove any surface oxidation and organic material, then rinsed with 100% ethyl alcohol and deionized water (DI) to ensure the surfaces and channels are clear of particles that may affect performance of the OHP. An indium wire was inserted into the rectangular groove along the outer edge of the bottom plate, and the two OHP halves were pressed together in a hydraulic press, crushing the indium wire, creating an air tight seal of the OHPs inner channels when the

fill pipe is closed. 34 individual nuts and bolts surround the edge of the OHP assembly, shown in Figure 2.2, and were tightened to ensure the two halves remain sealed during testing cycles.

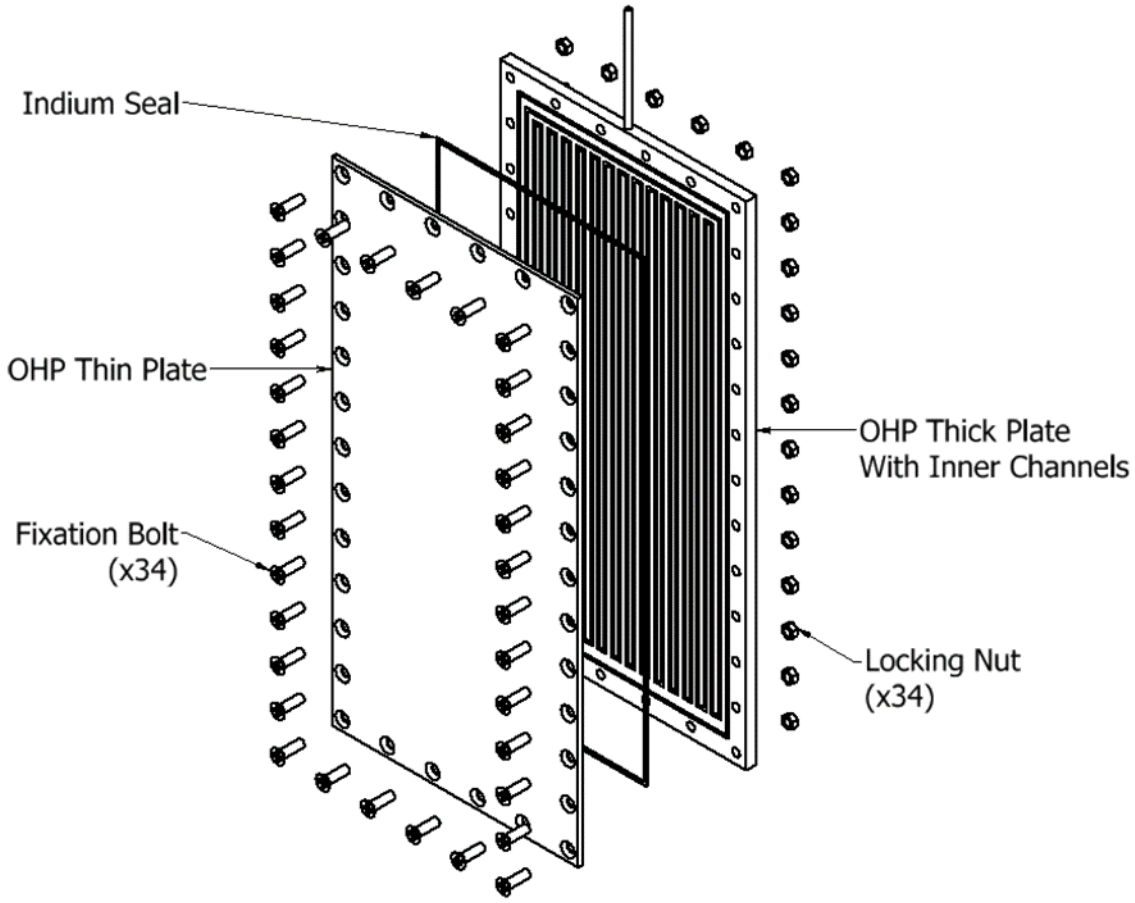

Figure 2.2. Exploded diagram of OHP assembly.

The fill tube is then attached to a vacuum-tested whitey valve, allowing for quick opening and sealing of the OHPs inner channels.

2.2 Charging Procedure

The OHP assembly was placed on a laboratory balance to closely monitor mass. The whitey valve of the OHP was then connected to a vacuum pump system that allows for the

evacuation and charging of the OHP internals. The valve was opened, and vacuum pump ran for approximately two hours, until the internal vacuum of the OHP read ~0.15 Torr, the lower limit of the vacuum pump assembly. Once an acceptable vacuum level was reached, the OHP valve was closed and the mass of the OHP assembly recorded. The vacuum pump assembly was then disconnected from the OHP, and HPLC grade water was injected into the evacuated internals of the OHP via a tube connected to the whitey valve. Once the OHP was full of HPLC grade water, its mass was recorded as the charged OHP mass. This mass, minus the evacuated mass of the OHP, resulted in the mass of water inside the OHP assembly.

$$WM = COM - EOM \tag{1.1}$$

Once the total mass of HPLC grade water inside the OHP assembly was known, multiplication by the fill percentage resulted in the desired water mass inside the OHP necessary to meet the target fill ratio, measured in percent water-by-mass.

$$DWM = WM \cdot FP \tag{1.2}$$

The desired water mass was then added to the evacuated OHP mass to determine the target mass of the OHP assembly. To achieve this target mass the OHPs whitey valve was connected to the vacuum pump assembly and slowly opened and closed to allow the vacuum pump to remove water from the interior of the OHP assembly. This process was done until the target mass was achieved, resulting in the target fill ratio of water inside the OHP.

$$TOM = EOM + DWM \tag{1.3}$$

To calculate the observed fill percentage the evacuated mass of the OHP assembly was subtracted from the observed mass of the OHP assembly and divided by the overall mass of the water.

$$OP = \frac{OOM - EOM}{WM} \tag{1.4}$$

This method of closing and opening the whitey valve to achieve the desired water mass does not allow for very precise evacuation of water from the OHP internals, so some error is inherent in this process.

2.3 Testing Setup

Five T-type thermocouples were used to measure temperatures of the OHP. Each thermocouple was tested to ensure accuracy, numbered from 6-10 to ensure accurate organization of data, and placed securely against the bottom plate of the OHP with 3M aluminum tape. Two thermocouples were placed directly under the evaporator section of the OHP, 20 mm from the edges of the OHP, and 20 mm apart from each other. Two thermocouples were also placed directly under the condenser section of the OHP, 20 mm from the edges and 20 mm apart. One final thermocouple was placed under the center of the adiabatic region of the OHP, 30 mm from the edges of the OHP and 33mm from the evaporator and condenser thermocouples. Figure 2.3 shows the placement of thermocouples on the OHP, and fixation with metallic tape.

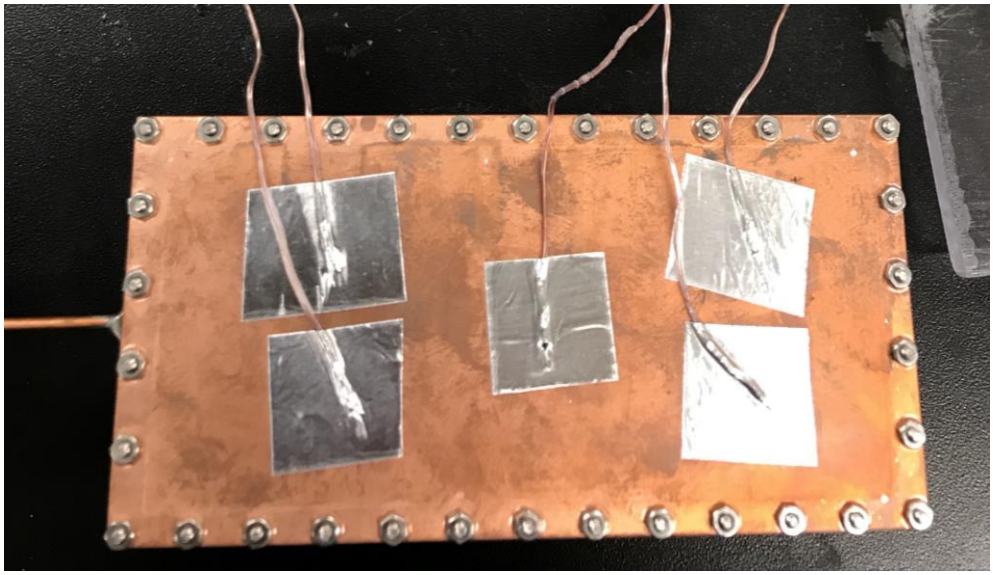

Figure 2.3. Thermocouple placement on bottom plate of OHP.

Once the thermocouples were secured against the OHP bottom plate, the OHP was placed on a large aluminum backing plate. Two fiberglass insulation pads were placed between the OHP bottom plate and aluminum backing plate to minimize any thermal effects the aluminum plate may have on the OHP. The whitey valve was then securely bolted to the aluminum backing plate to prevent movement of the fill tube. Aluminum heating and cooling blocks were covered in thermal paste and bolted to the top plate of the OHP, securing the OHP assembly to the aluminum backing plate, and ensuring thermal paste remains between the OHP plate and heating and cooling block assemblies. Cylindrical cartridge heaters were covered in thermal paste and inserted into cylindrical holes inside the heating block, creating an evaporator region on the OHP, wherein latent heat was added to the working fluid inside the OHP and removed from the cartridge heaters. These heaters are attached to an adjustable DC power supply where voltage and current was adjusted to generate the desired heat input to the OHP. Two three-foot cooling lines were attached from the cooling block to an industrial cooling bath, where temperature of the cooling liquid (water) was controlled and monitored. This cooling bath

pumped water through the cooling block on the OHP assembly, creating a condenser region on the OHP wherein latent heat was removed from the working fluid inside the OHP and transferred to the cooling bath liquid. Once the evaporator and condenser regions of the OHP were assembled, the aluminum backing plate was attached to an upright support, shown in Figure 2.4, with the OHP in the upright position, evaporator region directly below the condenser region.

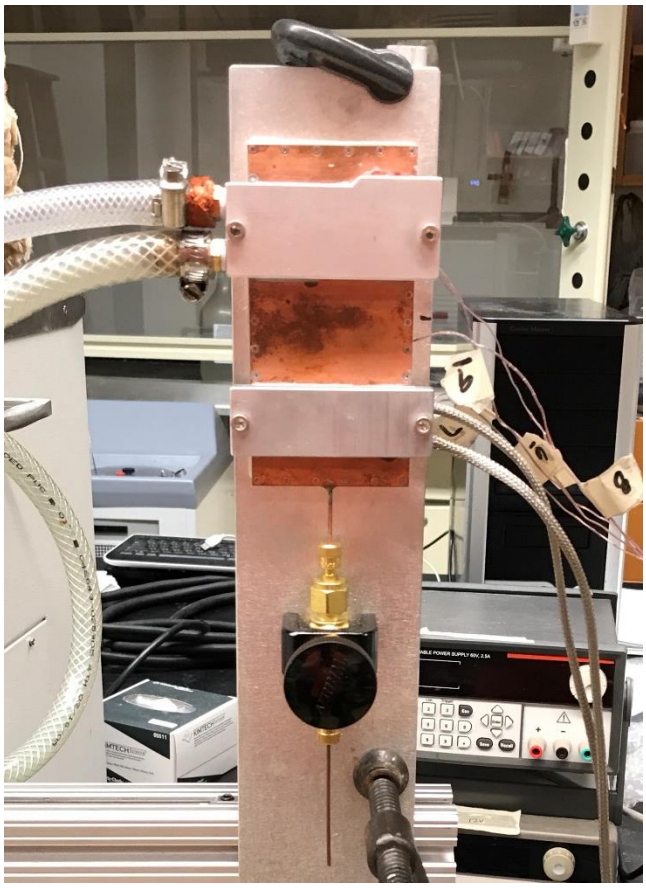

Figure 2.4. OHP assembly in final state, minus insulation.

Fiberglass insulation was then placed around the entire assembly, shown in Figure 2.5, and held together with string, to ensure that the OHP assembly, heating block, and cooling block were insulated from the atmosphere. Thermocouples were attached to a desktop computer, allowing for testing to begin and temperature data to be stored and analyzed.

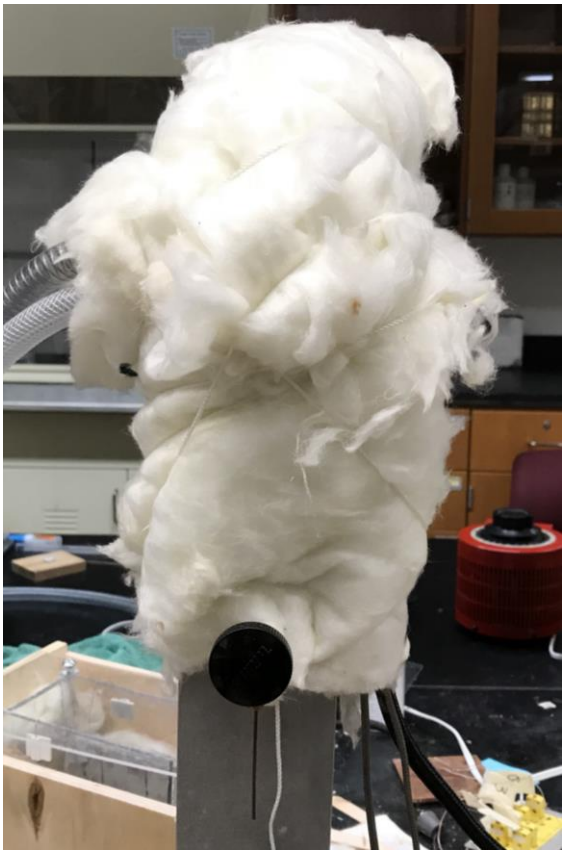

Figure 2.5. Final OHP assembly, notice fiberglass insulation and cooling lines.

2.4 Testing Procedure

Once the OHP assembly was complete, the cooling bath temperature and range of heat input provided by the cartridge heaters was determined. Cooling bath temperatures of 20 °C, 25 °C, 60 °C are used throughout testing to analyze the OHP performance over a wide range of condenser region temperatures. Heat input provided to the evaporator region of the OHP ranges from 10-280 W in intervals ranging from 10-30 W to ensure a variety of data is captured when the working fluid inside the OHP is in a non-oscillating, transition, or oscillating state. OHP fill ratio is set at 50% water-by-mass and 65% water-by-mass in order to provide a variety of data for comparison, as previous studies show that OHP performance is influenced by fill ratio.

Testing began once the desired cooling bath temperature is selected, water pump activated, cartridge heaters connected to their DC power supply, thermocouples attached to a desktop computer, and LabView Signal Express 2009 data analysis tools recording temperature data. All testing begins at 10 W of evaporator region heat input, log files of all five thermocouple readings are stored in a .txt file with data acquired at a rate of 100 Hz. Data logs of the transient temperature of the OHP begin with initial heat input, data is constantly acquired until the temperature readings from all five thermocouples enters a constant state. Logs of constant temperature data are acquired once the temperature readings of the thermocouples enter steady state, three minutes of temperature data from each thermocouple are saved in a .txt file. Testing ceased once all thermocouple data is acquired, in both transient and constant regions of thermocouple temperatures, from evaporator heat input of 10 W through approximately 280 W.

2.5 Nam-Ju Oxidation Procedure

Created by Youngsuk Nam and Y. Sungtaek Ju, the Nam-Ju copper (II) oxide is a nanostructured oxide that increases surface roughness of the copper. The Nam-Ju oxide is shown to reduce the contact angle of a water droplet to approximately 20°, down from 60° on untreated copper [11], increasing wettability of copper and influencing fluid movement inside the OHP.

Once final testing of the natural oxide OHP was complete, the OHP is completely disassembled. The indium seal is removed and copper halves of the OHP were scrubbed with a wire brush. Both halves of the OHP assembly were then washed with 2.0 M HCl, 100% ethyl alcohol, and DI water to remove any organic materials or oxidation. Once washed, the OHP halves were placed into a solution containing 200 mL DI water, 7.55 g $NaClO_2$, 10.05 g NaOH,

and 20.06 g $Na_3PO_4 \cdot 12H_2O$ and heated to 95 °C. The OHP halves remained in the solution for approximately 10 minutes, while the solution is stirred every 30 seconds. After the 10-minute bath is complete, the OHP halves appeared dark black in color, shown in Figure 2.6, indicating that the Nam-Ju oxide has been applied to the surface.

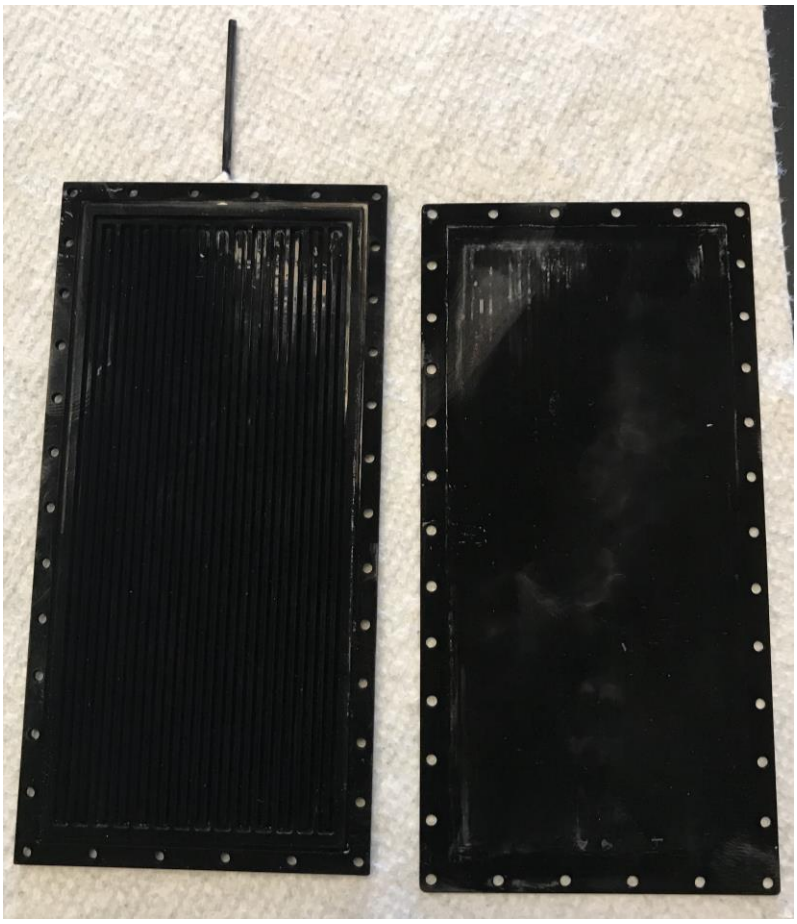

Figure 2.6. Nam-Ju copper (II) nanostructure oxidized OHP halves.

The OHP halves were removed and immediately soaked in DI water to halt the oxidation process. The halves were then left to air dry, before being reassembled into the complete OHP assembly. Reassembly follows a similar process as assembly, the exception being that a wire brush was used to remove the Nam-Ju oxide from the indium wire groove on the bottom plate, and top plate edges. The Nam-Ju oxide was removed from the groove as a precaution, it was unknown whether the Nam-Ju oxide prevents the indium from sealing correctly, but removal of the Nam-Ju oxide from the edges of the plate does not affect the OHP inner channels. Once complete, the assembly procedure continued, the indium wire was placed into the respective groove, a hydraulic press used to deform the wire, and the 34 nuts and bolts prevent the halves from separating. The OHP was then charged to a desired ratio of water-by-mass and assembled for testing, shown in Figure 2.7.

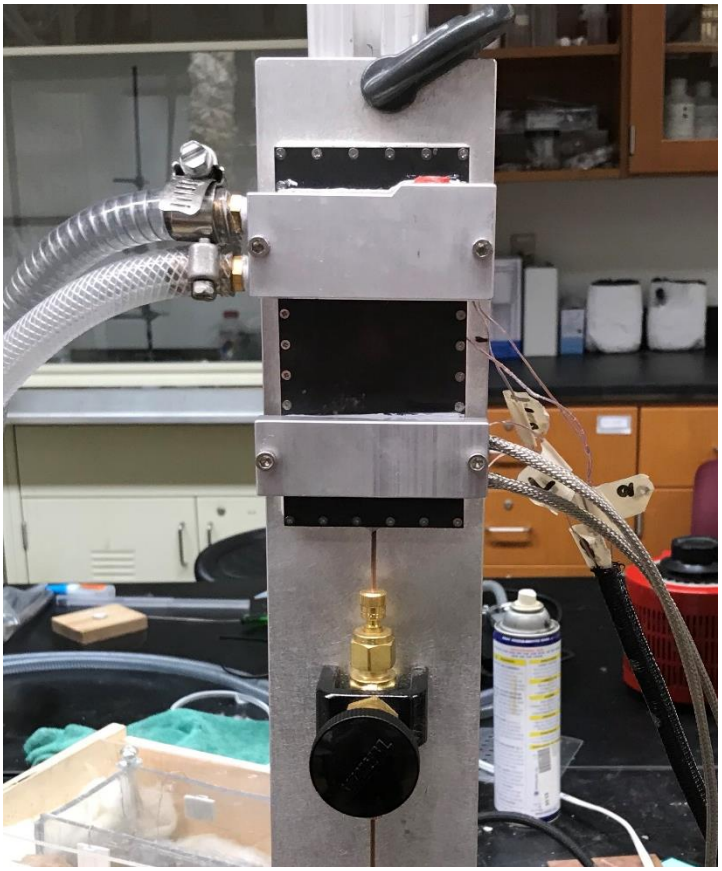

Figure 2.7. Assembled Nam-Ju oxidized OHP, minus surrounding fiberglass insulation.

3 Evacuated OHP Testing

To provide baseline comparison, the OHP was fully evacuated and setup for testing following procedures stated in sections 2.2 and 2.3. Evaporator heat input of 10-280 W was selected to provide data on the difference in temperature from the evaporator and condenser regions, through a wide range of heat fluxes. However, testing could not continue beyond 135 W of heat input, due to limitations of the OHP assembly. The OHP's two-piece nature requires the indium seal to maintain a closed environment, and while indium is a soft metal that readily deforms inside the seal groove around the edge of the OHP, it has a melting point of 156.6 °C. To ensure the indium seal does not melt, breaking the vacuum seal and exposing the inner channels of the OHP to the surrounding environment, maximum temperature limits were set at 125 °C, measured at the thermocouples attached to the base of the OHP.

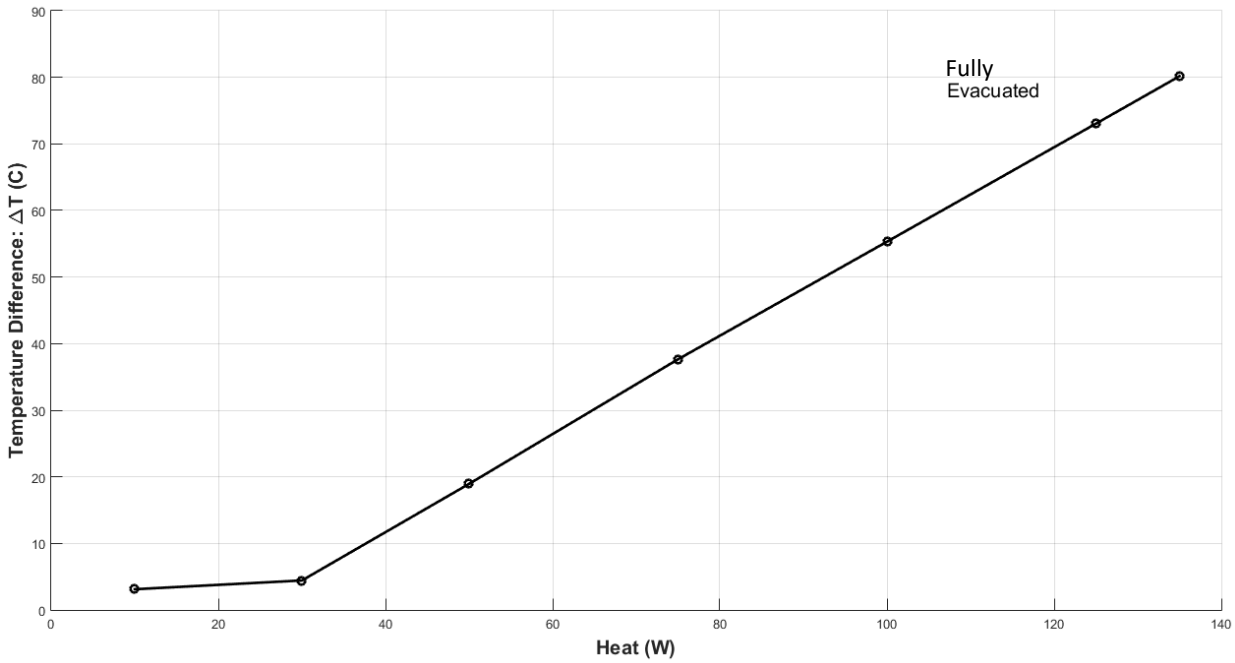

Figure 3.1. Temperature difference between evaporator and condenser regions vs heat input of full evacuated (0.0% charged) OHP with 25 °C cooling bath.

Testing ceased at 135 W of heat input, as the thermocouples beneath the evaporator region of the OHP reached temperatures of over 125 °C. For much of the data, temperature difference between the evaporator and condenser regions of the OHP rises at a constant rate, with respect to heat input supplied, as expected from pure conduction through a flat copper plate. However, from 10 W through 30 W of heat input there is a low increase in temperature difference, significantly lower than the rest of the data. While the reason behind this non-constant rise in temperature difference is unknown, it is theorized that the OHP does not act as a flat plate of copper, instead acting as two separate plates separated by a vacuum, shown in Figure 3.2, and with limited points of contact, primarily the edges of the plates and ridges separating the grooves.

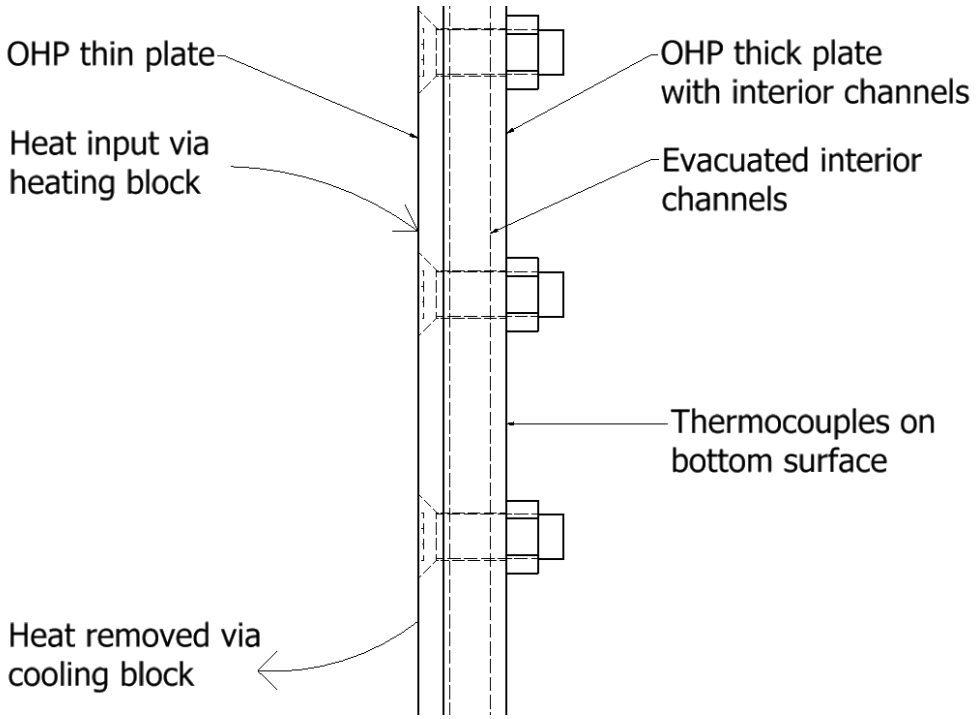

Figure 3.2. OHP side-view, the two-piece assembly with evacuated inner region may not act as a solid plate of copper, allowing heat to spread in a non-uniform path.

Because of this separation and limited contact, it is possible that low levels of heat travel more readily through the thin (top) plate of the OHP, allowing for greater heat exchange between

the evaporator and condenser regions of the thin plate, while limiting heat input to the thick (bottom) plate of the OHP, which contact the thermocouples and allow for temperature monitoring. Once 50 W of heat input is provided to the evaporator region, heat readily travels through the thick plate, and the thermocouples record a large, and constant rise in temperature with respect to heat input. This large and constant increase in temperature difference with respect to heat input is expected with a pure conduction mode of heat transport and allows for a basic comparison between the OHP when charged with a mixture of water, and a flat plate of copper of the same volume and mass, under identical testing conditions.

4 Natural Oxide OHP Testing

Initial testing began with the OHP in its natural oxide state, machined copper internals with no surface treatment. Previous studies show that fill ratios affect OHP performance [9] so fill ratios of 50% and 65% water-by-mass are selected for use to provide a variety of data. Heat supplied to the evaporator region of the OHP ranges from 10-280 W, allowing for thermal performance measurements over a wide range of heat fluxes. Condenser region cooling bath temperatures of 20 °C, 25 °C, and 60 °C were selected to provide a variety of data regarding how the OHP would perform over a wide condenser temperature range.

4.1 50 Percent Water-by-Mass Tests

Repeatability was the focus of the initial OHP testing, to ensure the setup allows for consistent results under identical conditions, and to ensure the OHP seal did not rupture at high temperatures or pressures. The target fill ratio of 50% water-by-mass, condenser temperature of 25 °C, and evaporator heat input range of 10-280 W were selected for initial OHP testing. The observed OHP fill ratio was 49.9%. Beginning at 10 W, 10 W intervals of heat input were

selected until the working fluid inside the OHP began to move. Upon oscillation of working fluid, detected by a decrease in the rise of temperature difference between the evaporator and condenser regions, and the increase in fluctuation of temperature readings in the evaporator region, the interval of heat input increased to 20 W. Two trials commenced on separate dates, with identical cooling bath temperatures and heat inputs.

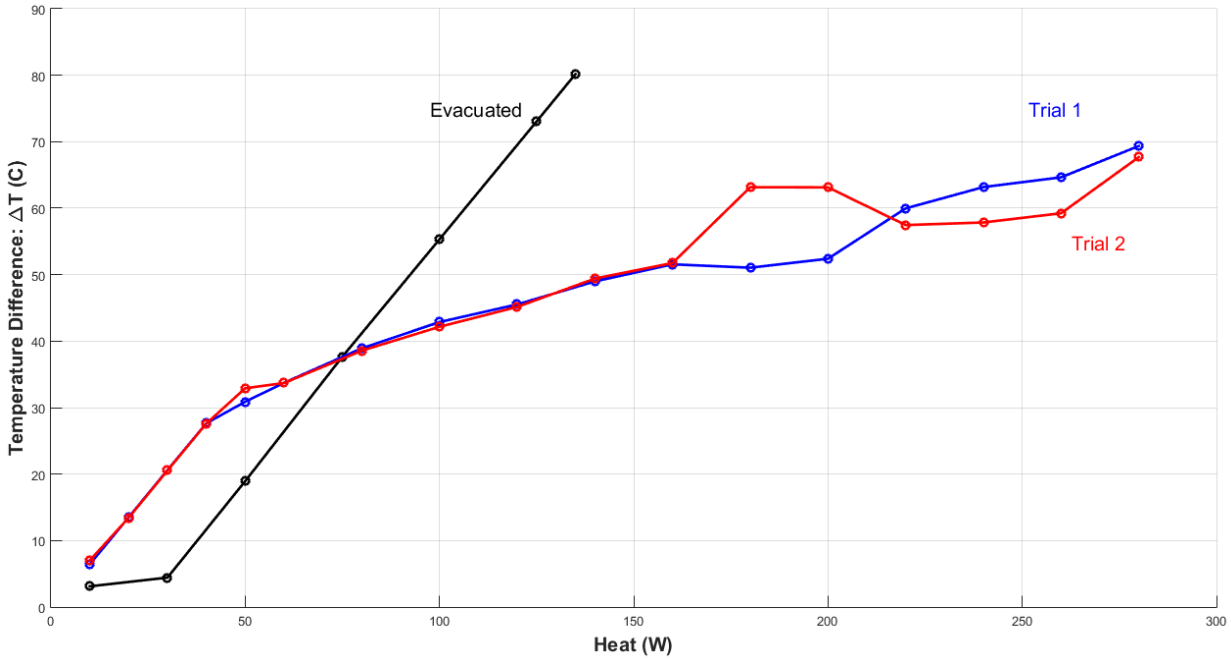

Figure 4.1. Temperature difference between evaporator and condenser regions vs heat input of the evacuated OHP, Trial 1 (50% charged OHP), and Trial 2 (50% charged OHP) with a 25 °C cooling bath.

In the non-oscillating region of OHP trials 1 and 2, between 10 W and 50 W of evaporator heat input, the rate of temperature difference between the evaporator and condenser regions is constant. Once the working fluid inside the OHP begins movement, at approximately 60 W of heat input, a decrease in temperature difference between the evaporator and condenser regions is observed. This difference is consistent in both trials between 60 W and approximately 160 W, upon which a region of disturbance is observed at 180 W, lasting until approximately 220 W, at which time the rate of increase in temperature difference of the two trials becomes consistent. The behavior of the OHP and temperature differences between evaporator and

condenser regions is consistent, providing reasonable evidence that future OHP tests are repeatable, and thus data acquired from the OHP testing is comparable. Upon completion of the initial trials, tests began with cooling block temperatures of 20 °C, 25 °C, and 60 °C.

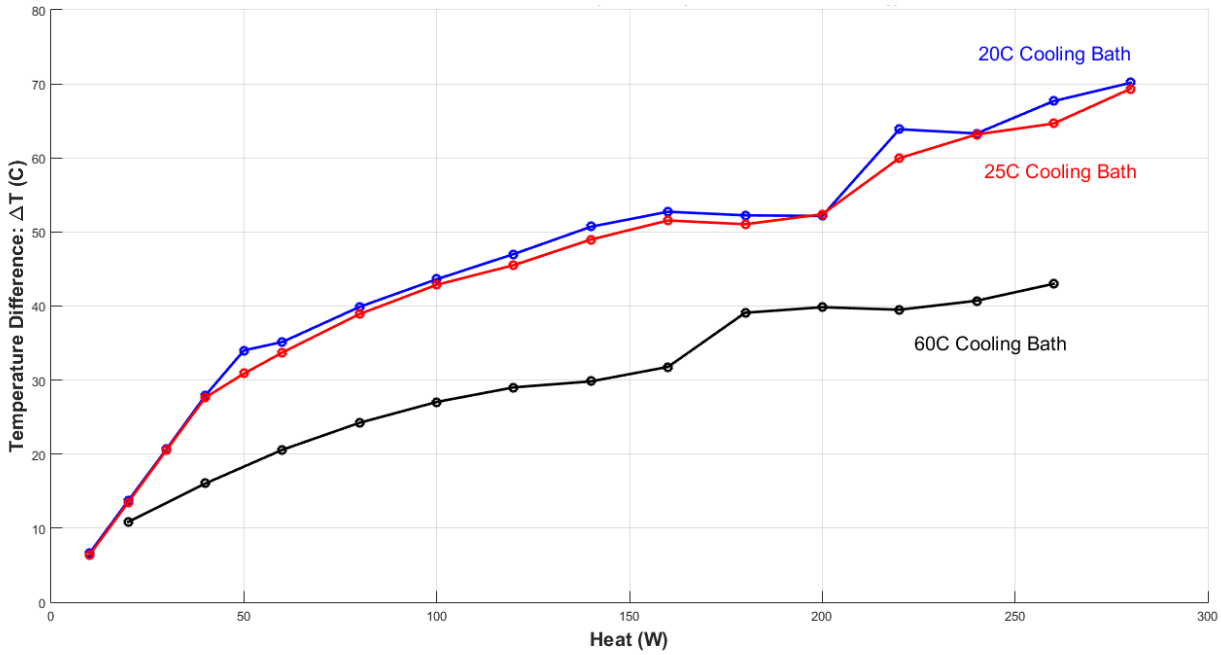

Figure 4.2. Temperature difference between evaporator and condenser regions vs heat input of 50% charged OHP with 20 °C, 25 °C, and 60 °C cooling baths.

Figure 4.2 shows the results of the 50% water-by-mass OHP assembly performance at three different cooling block temperatures. The basic profile of each temperature difference curve is similar, however the 60 °C cooling bath test undergoes working fluid oscillation with as low as 20 W of heat input. The 20 °C cooling bath resulted in a larger temperature difference between the evaporator and condenser regions of the OHP, peaking at 70.2 °C, while the 60 °C cooling bath resulted in the smallest temperature difference, peaking at 43.0 °C. The 60 °C cooling bath test ended prematurely at 260 W, as evaporator temperatures began to rise near the melting point of the indium seal.

4.2 65 Percent Water-by-Mass Tests

Following the repeatability and initial results of the 50% fill ratio OHP testing, the OHP was evacuated and charged to 65.8% water-by-mass, meeting the target fill ratio of 65%. Cooling bath temperatures of 20 °C, 25 °C, and 60 °C were again selected, and the OHP was tested over the desired input heat interval of 10-280 W.

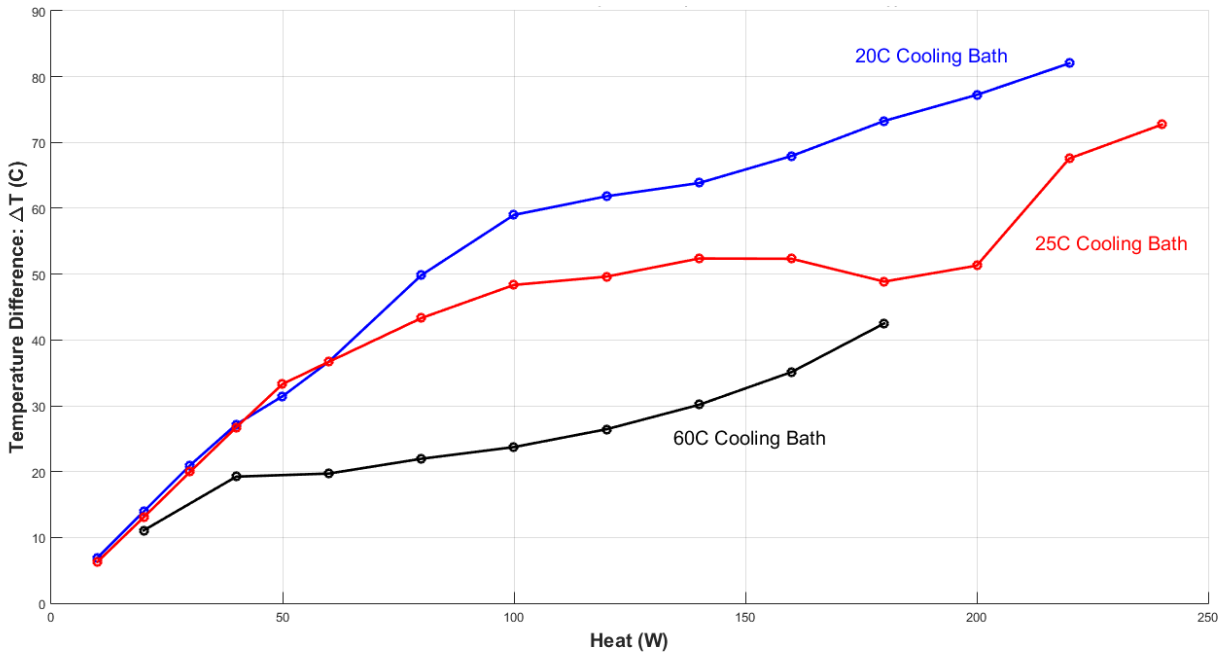

Figure 4.3. Temperature difference between evaporator and condenser regions vs heat input of 65% charged OHP with 20 °C, 25 °C, and 60 °C cooling baths.

Figure 4.3 shows the results of OHP testing, with trends similar to those of the 50% fill ratio OHP tests. Again, the 20 °C cooling bath resulted in the highest difference in temperature between the evaporator and condenser regions of the OHP, peaking at 82.0 °C, while the 60 °C cooling bath resulted in the lowest maximum temperature difference, peaking at 42.5 °C. However, the maximum heat input of 280 W was never reached in any of the three tests. Testing

ended prematurely to protect the integrity of the indium seal, as evaporator temperatures neared the melting point of indium.

5 Nam-Ju Oxidized OHP Results

Upon completion of natural oxide OHP testing, the OHP was disassembled, the Nam-Ju oxide applied to the interior surfaces following procedure stated in section 2.5, reassembled, and charged to a target fill ratio. 50% and 65% HPLC water-by-mass fill ratios and cooling bath temperatures of 20 °C, 25 °C, and 60 °C were selected for initial testing of the Nam-Ju oxidized OHP. These fill ratios and cooling bath temperatures are identical to those tested with the natural-oxide OHP, allowing for accurate performance comparisons between a natural copper oxide OHP and Nam-Ju oxidized OHP.

5.1 50 Percent Water-by-Mass Tests

Following previous testing guidelines with the natural oxide OHP, the target fill ratio of 50% water-by-mass and condenser temperature of 20 °C were selected. The obtained OHP fill ratio was 49.9%, meeting the 50% target fill ratio. However, the range of heat input varies when compared to previous testing, down to 10-260 W from 10-280 W to protect the indium seal from possible damage, as signs of melting indium occurred after previous testing to 280W. Beginning at 10 W, 10 W intervals of heat input were selected until the working fluid inside the OHP began to oscillate, at approximately 40 W. Upon oscillation of working fluid, the interval of heat input increased to 20 W. Once 80 W of heat input is reached, the interval decreases to 10 W, to provide more data points as the oscillation inside the OHP intensifies. Upon reaching 100 W of heat input, the interval increases to 20 W for two more data points, increasing again to 30 W upon reaching 140 W of total heat input. Testing ceases at 260 W of heat input and the OHP

assembly is cooled to room temperatures before further testing at cooling bath temperatures of 25 °C and 60 °C can begin. The comparison of natural oxide OHP and nano-oxide OHP results, at 50% water-by-mass and a 20 °C cooling bath temperature, are visible in Figure 5.1.

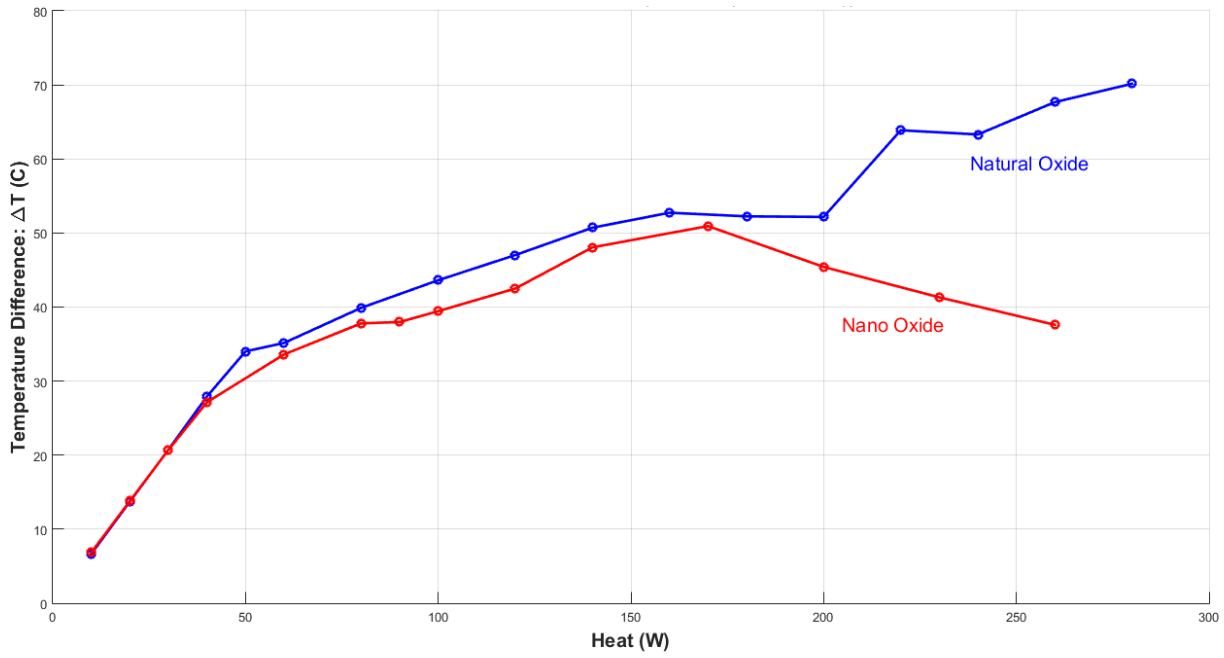

Figure 5.1. Temperature difference between evaporator and condenser regions vs heat input of 50% charged natural oxide OHP and Nam-Ju oxidized OHP with 20 °C cooling bath.

During initial heating of the OHP assemblies, from 10-40 W, the temperature difference vs heat input is linear, but as fluid begins to oscillate inside the OHP assemblies, the Nam-Ju oxide OHP shows a further reduction of temperature difference between evaporator and condenser regions. This reduction in temperature difference over the natural oxide OHP continues throughout the rest of testing, resulting in a downward trend as the heat input increases beyond 170 W of heat input. The maximum performance increase of the Nam-Ju oxidized OHP occurs at 260 W of heat input, the temperature difference between the evaporator and condenser regions of the Nam-Ju oxidized OHP is 30.1 °C cooler than the natural oxide OHP, a reduction

of 44.5%. Further testing is done with cooling bath temperatures of 25 °C, the comparison and results are shown in Figure 5.2.

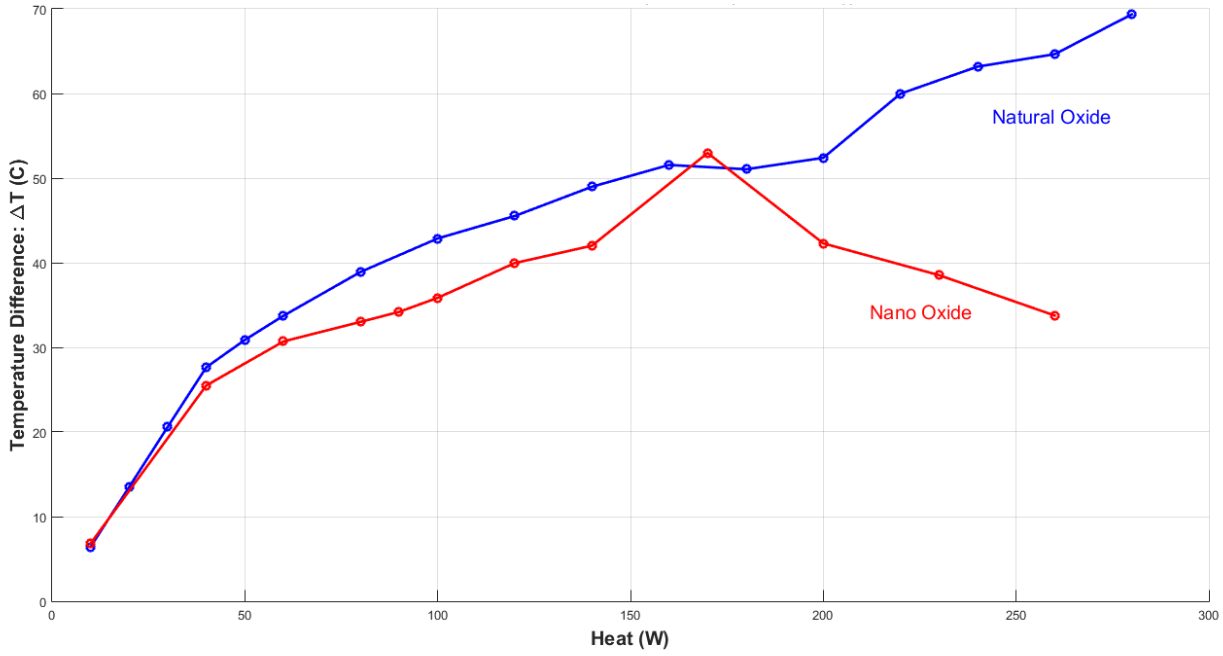

Figure 5.2. Temperature difference between evaporator and condenser regions vs heat input of 50% charged natural oxide OHP and Nam-Ju oxidized OHP with 25 °C cooling bath.

The results of the 25 °C cooling bath testing is consistent, with linear temperature difference with heat input during initial heating from 10-40 W, decreased temperature difference upon working fluid oscillation, and further decreasing temperature difference of the Nam-Ju oxidized OHP upon exceeding heat inputs of 170 W. The maximum performance increase of the Nam-Ju oxidized OHP occurs at 260 W of heat input, where the Nam-Ju oxidized OHP temperature difference is 30.8 °C less than the temperature difference of the natural oxide OHP, a 47.7% reduction. Further testing is done with cooling bath temperatures of 60 °C, the comparison and results are shown in Figure 5.3.

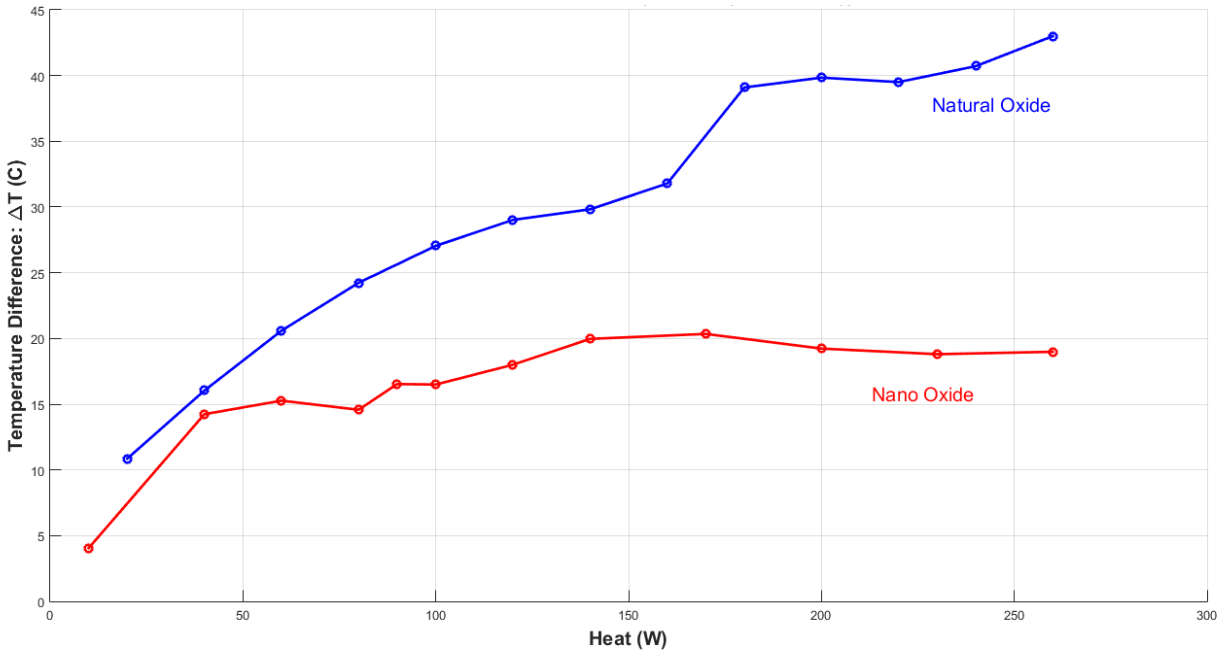

Figure 5.3. Temperature difference between evaporator and condenser regions vs heat input of 50% charged natural oxide OHP and Nam-Ju oxidized OHP with 60 °C cooling bath.

The 60 °C cooling bath test shows further performance improvement, with the Nam-Ju oxidized OHP maintaining the same trends as in Figure 5.1 and Figure 5.2, with significantly lower temperature differences than seen in the natural oxide OHP testing. The maximum performance increase of the Nam-Ju oxidized OHP again occurs at 260 W of heat input, where the temperature difference between the evaporator and condenser regions of the Nam-Ju oxidized OHP is 22.6 °C less than the temperature difference of the natural oxide OHP, a 52.6% reduction. One note of interest however is the reduction in temperature difference of the Nam-Ju oxidized OHP at the initial stage of OHP testing, 10-40 W of heat input. Figure 5.1 and Figure 5.2 show the Nam-Ju oxidized OHP and natural oxide OHP having nearly identical temperature differences until the working fluid begins to oscillate. However, the 60 °C cooling bath tests show working fluid oscillation with heat inputs as low as 20 W, therefore the reduction of

temperature difference on the Nam-Ju oxidized OHP, in the initial regions of heat input, is expected.

5.2 65 Percent Water-by-Mass Tests

Following the procedures in section 2.4 and 2.5, the OHP was evacuated and recharged to 62.8% water by mass, meeting the target fill ratio of 65%. Testing follows established procedure, in which the cartridge heaters attached to the evaporator region of the OHP receive a heat input ranging from 10-280 W, up from the 10-260 W interval used in the tests involving the Nam-Ju oxidized OHP with a 50% fill ratio. Cooling bath temperatures of 20 °C, 25 °C, and 60 °C were again selected, with testing to begin with a 20 °C cooling bath.

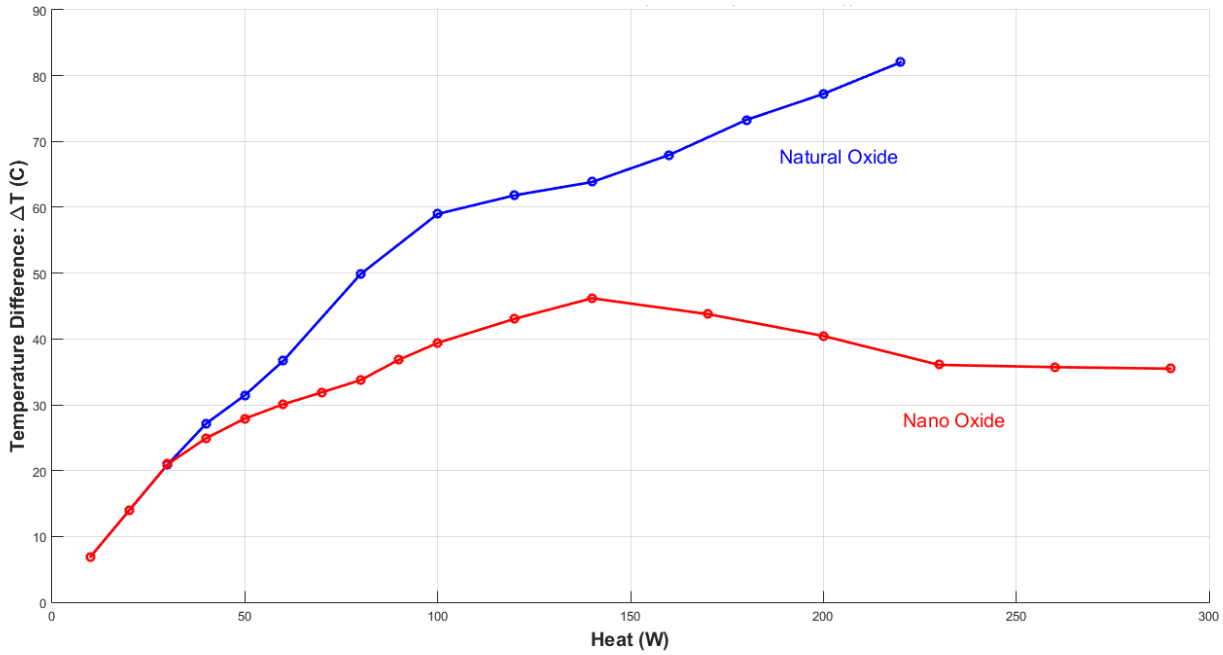

Figure 5.4. Temperature difference between evaporator and condenser regions vs heat input of 65% charged natural oxide OHP and Nam-Ju oxidized OHP with 20 °C cooling bath.

Figure 5.4 shows the results of the 65% fill ratio Nam-Ju OHP vs the 65% charged natural oxide OHP, with a 20 °C cooling bath. Initial heat input from 10-30 W resulted in nearly

identical temperature differences between the evaporator and condenser regions of the Nam-Ju oxidized OHP and natural oxide OHP, however temperatures begin to rise at a lower rate with further heat input to the nano-oxide OHP. The maximum temperature difference between the evaporator and condenser regions of the nano-oxide OHP peaks at 46.2 °C and 140 W of heat input, before reducing as further heat is added. This follows the trends established by the previous 50% fill tests, in which the temperature difference peaks before a slight decline towards maintaining temperature difference levels with added heat input. The maximum performance increase of the 65% fill ratio Nam-Ju oxidized OHP occurs at 230 W of heat input, where the temperature difference between the evaporator and condenser regions of the Nam-Ju oxidized OHP is approximately 44.5 °C less than the temperature difference of the natural oxide OHP, a 54.3% reduction. Testing continues with a cooling bath temperature of 25 °C, with the comparison and results shown in Figure 5.5.

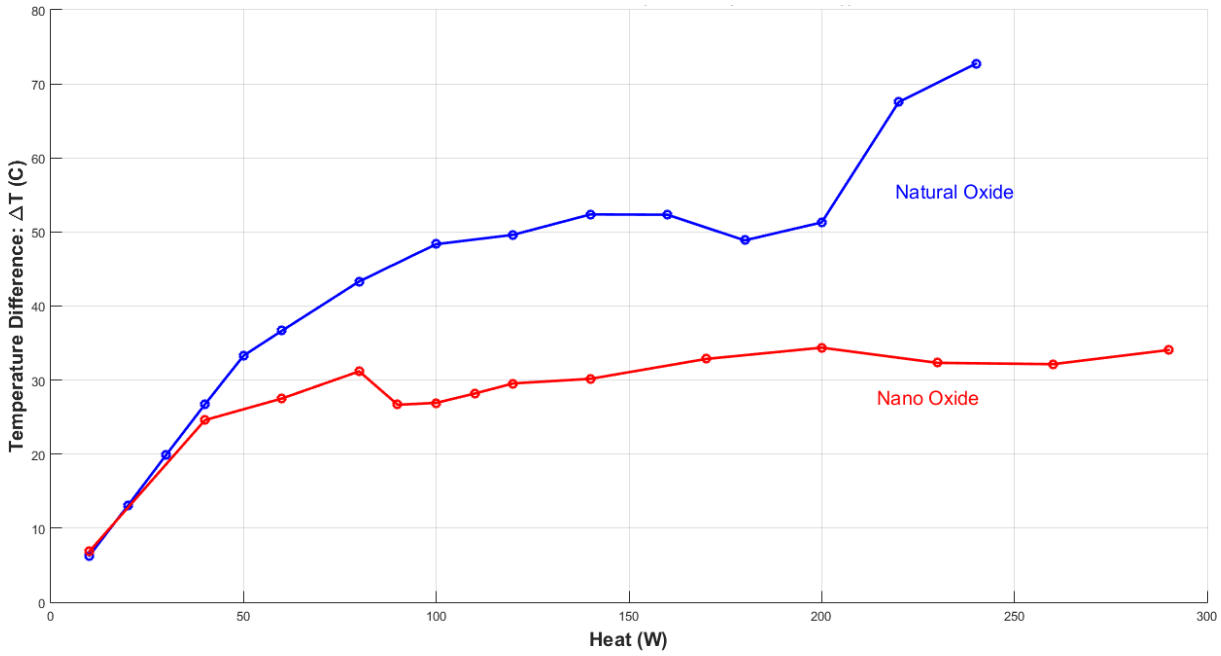

Figure 5.5. Temperature difference between evaporator and condenser regions vs heat input of 65% charged natural oxide OHP and Nam-Ju oxidized OHP with 25 °C cooling bath.

The results of the 25 °C cooling bath test are consistent with previous test trends, in which the Nam-Ju oxidized OHP has significantly reduced temperature differences when compared to the natural oxidized OHP. The maximum performance increase of the 65% fill ratio Nam-Ju oxidized OHP occurs at 240 W of heat input, the temperature difference between the evaporator and condenser regions of the Nam-Ju oxidized OHP is 40.4 °C cooler than the natural oxide OHP, a reduction of 55.6%. Further testing is done with cooling bath temperatures of 60 °C, the results of which are shown in Figure 5.6.

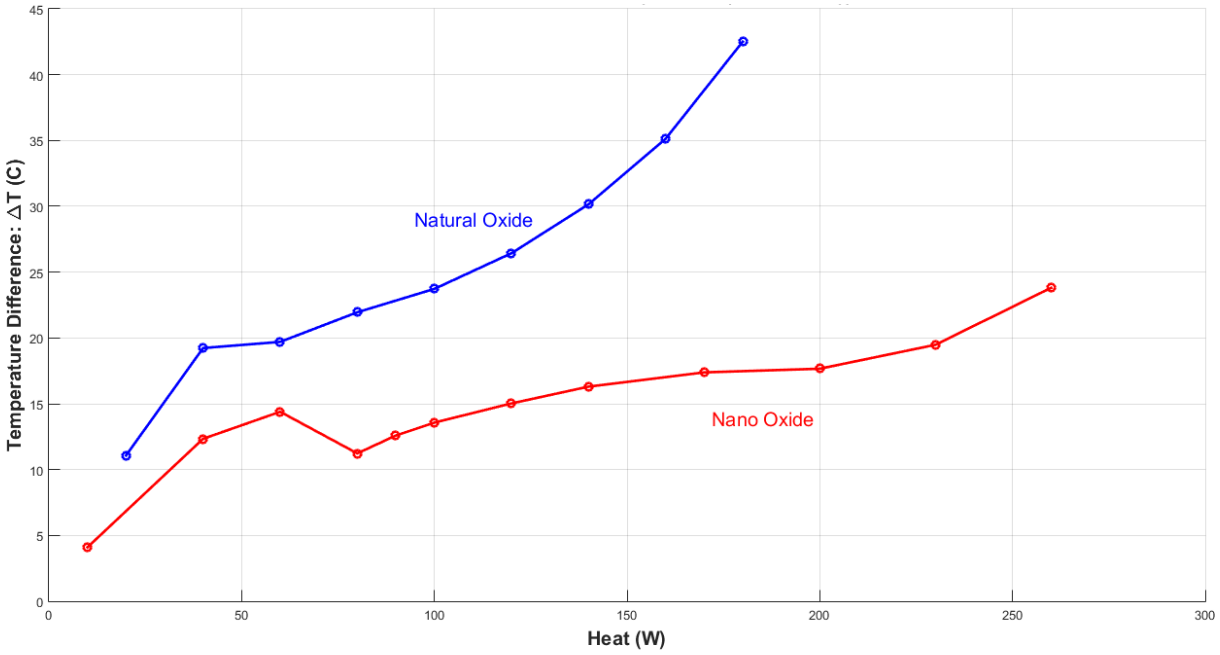

Figure 5.6. Temperature difference between evaporator and condenser regions vs heat input of 65% charged natural oxide OHP and Nam-Ju oxidized OHP with 60 °C cooling bath.

The 60 °C cooling bath test follows trends established by previous 60 °C cooling bath tests. In the initial heat input interval, 10-40 W, the Nam-Ju oxidized OHP shows reduced temperature difference, when compared to the natural oxide OHP. This reduction in temperature difference over the initial 10-40 W heat interval may be explained by the working fluid

oscillating at heat inputs as low as 20 W when the cooling bath is set to 60 °C. The maximum performance increase of the 65% fill ratio Nam-Ju oxidized OHP occurs at 180 W of heat input, the temperature difference between the evaporator and condenser regions of the Nam-Ju oxidized OHP is 25.1 °C cooler than the natural oxide OHP. The result of such a drop in temperature difference is the largest performance increase of all tests in this experiment, a reduction of 59.1%.

5.3 Standard Deviation

Previous studies show that cupric oxide nanostructures influence the movement of working fluid inside of an OHP. This increase in fluid movement is implied by an increase in fluctuations of temperatures recorded by the thermocouples. Figure 5.7 shows a comparison between temperature fluctuations at 200 W heat input in the natural oxide OHP vs temperature fluctuations at 200 W heat input in the Nam-Ju oxidized OHP.

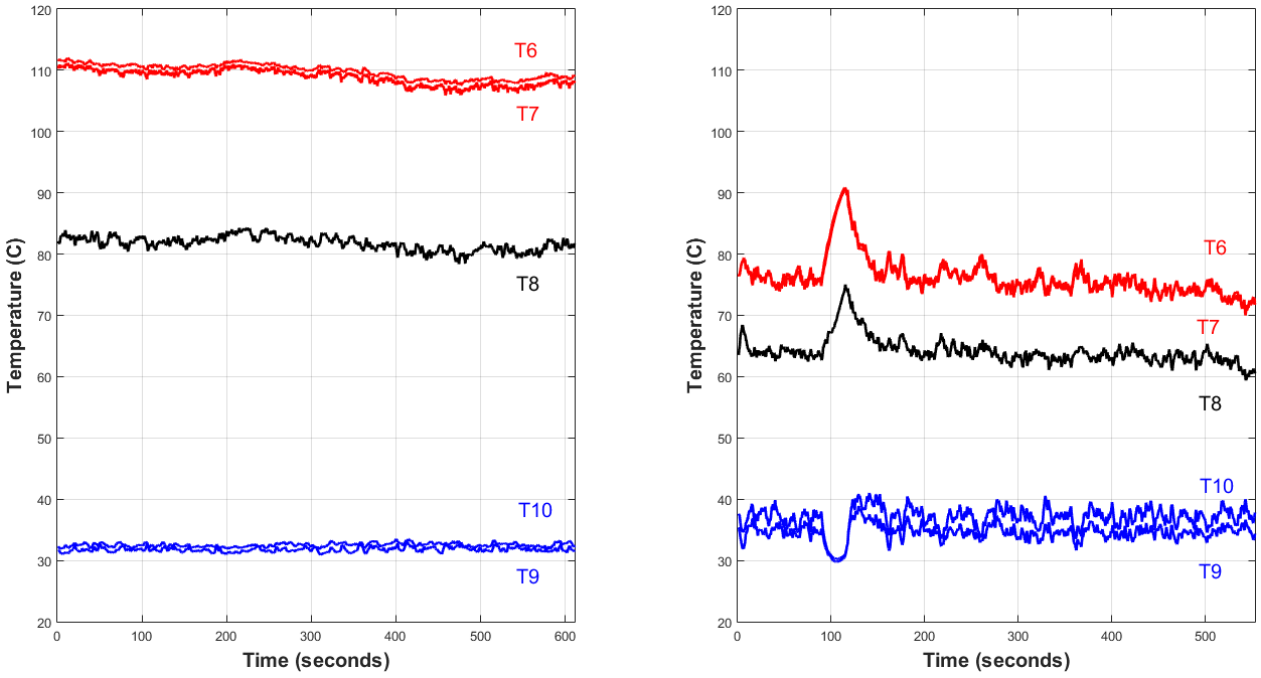

Figure 5.7. Thermocouple readings of natural oxide OHP at 200 W heat input and 20 °C cooling bath (left) compared to thermocouple readings of Nam-Ju oxidized OHP at 200 W heat input and 20 °C cooling bath (right), with thermocouples labeled T6-T10.

Figure 5.7 shows a significant increase in temperature fluctuation in the Nam-Ju oxidized OHP when compared to the natural oxide OHP. To quantify the increase in temperature fluctuation, and therefore fluid movement, the standard deviation of thermocouple data was acquired through the range of heat input to the OHP. The thermocouple data was then averaged to create an average standard deviation of all thermocouple data at each specified heat input. The average standard deviation of all thermocouple data is plotted against heat input in Figure 5.8, to compare temperature fluctuation, thus fluid movement, inside the natural oxide OHP and Nam-Ju oxide OHP.

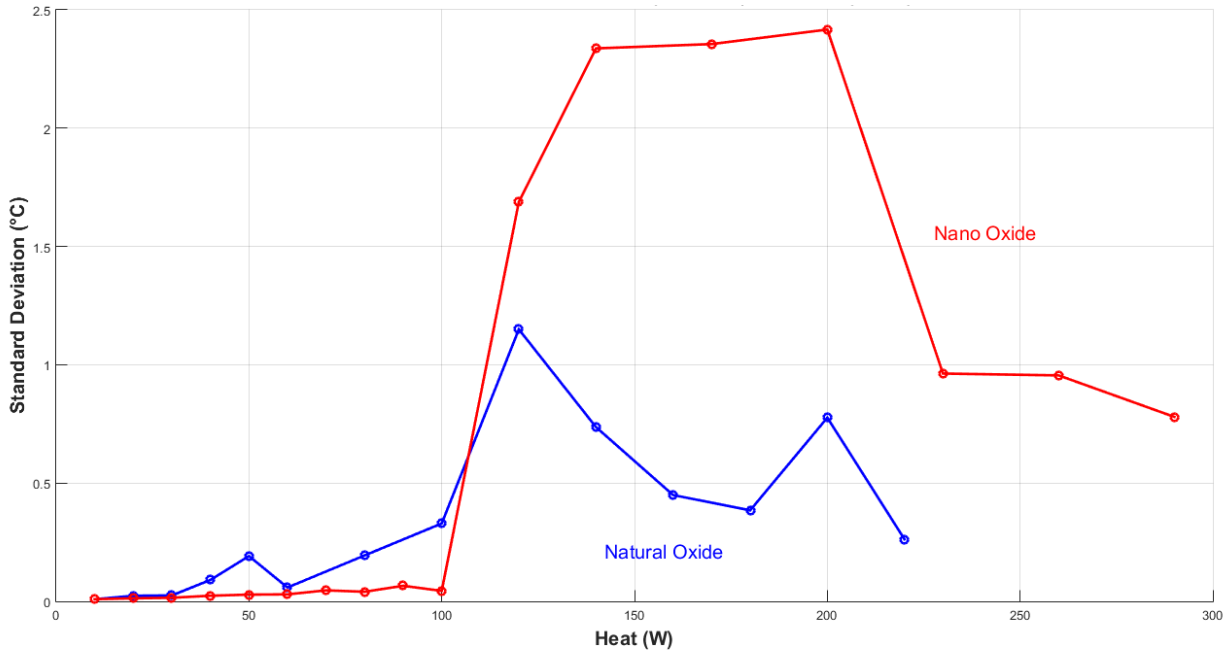

Figure 5.8. Average standard deviation of evaporator and condenser regions vs heat input of 65% natural oxide OHP and Nam-Ju oxidized OHP with 20 °C cooling bath.

During initial heat input, 0-100 W, fluctuations in temperature are low, reflected by the low standard deviations of both the Nam-Ju oxidized OHP and natural oxide OHP temperature readings, visible in Figure 5.8. However, as heat is added to the evaporator region, standard deviation increases rapidly, with the Nam-Ju oxidized OHP having up to an 80.9% increase in average standard deviation of temperature readings over the natural oxide OHP. While this increase in standard deviation is significant, and other tests also show that the Nam-Ju oxidized OHP has significantly higher standard deviation of temperatures, the causation behind the increased temperature fluctuations, and therefore increased fluid movement, can not be determined.

6 Conclusion

6.1 Summary

An experiment was conducted to determine if the Nam-Ju oxide influences the thermal performance of a closed loop, flat plate, oscillating heat pipe. The OHP was initially tested in its natural oxide state, with fill ratios of 50% and 65% HPLC grade water-by-mass selected for use as the working fluid inside the OHP. A cooling block and heating block were attached to the top OHP surface, five thermocouples were attached to the bottom OHP surface. The cooling block connected to a cooling bath with the temperature set to 20 °C, 25 °C, or 60 °C and heat input provided to the cartridge heaters inside the heating block ranged from 10-280 W. Temperatures were captured from the thermocouples and recorded over time, with log files saved for every change in heat input. Temperature differences between the evaporator and condenser regions of the OHP were analyzed, and plots of temperature difference vs heat input supplied to the evaporator region were created. The OHP was then disassembled, cleaned, and the Nam-Ju oxide layer applied evenly to the interior and exterior surfaces. The OHP was reassembled for testing in it's Nam-Ju oxidized state. Fill ratios of 50% and 65% HPLC grade water-by-mass were selected to allow for accurate comparisons to be made against previous natural oxide OHP testing. Cooling bath temperatures were set to 20 °C, 25 °C, and 60 °C, and thermocouples were attached to the bottom of the OHP thick plate. Testing commenced in a similar manner as with the natural oxide OHP. Once the heat input reached a level required for working fluid movement, the Nam-Ju oxidized OHP saw reductions in temperature difference between the evaporator and condenser regions, up to 59.1%, when compared to natural oxide OHP results.

6.2 Conclusions

Fill-ratio of the OHP affects the thermal performance, with the 50% water-by-mass fill ratio OHP resulting in reduced temperature difference between evaporator and condenser regions. The performance of the OHP is repeatable, with data acquired from multiple tests on separate days resulting in similar thermal performance. The application of the Nam-Ju nanostructure oxide to the OHP results in increased performance by reducing temperature differences between the evaporator and condenser regions of the OHP. The maximum performance improvements for each test of the natural oxide OHP and Nam-Ju oxidized OHP visible in Table 1.1

OHP Information	**Maximum Increase in Performance with Nam-Ju Oxide Applied**
50% Charged OHP	
20 °C cooling bath	44.5%
25 °C cooling bath	47.7%
60 °C cooling bath	52.6%
65% Charged OHP	
20 °C cooling bath	54.3%
25 °C cooling bath	55.6%
60 °C cooling bath	59.1%

Table 1.1. Maximum OHP performance increase for each test.

Standard deviations of thermocouple readings are significantly greater in the Nam-Ju oxidized OHP, implying that there is increased movement of the working fluid inside the Nam-

Ju oxidized OHP. The increase in performance is greater at higher cooling bath temperatures, with tests utilizing a 60 °C cooling bath showing the greatest performance.

6.3 Future Work

The mechanism behind the reduction of temperature difference between the evaporator and condenser regions of the OHP remains unclear. Future studies may utilize neutron imaging to analyze working fluid movement inside the OHP.

References

1. Akachi, H. (1990). “Structure of a Heat Pipe.” U.S. Patent #4,921,041.

2. Tong, B. Y., Wong, T. N., & Ooi, K. T. (2001). “Closed-loop pulsating heat pipe.” *Applied Thermal Engineering*, *21*(18), 1845–1862.

3. Cheng, P., & Ma, H. (2011). “A mathematical model of an oscillating heat pipe.” In *Heat Transfer Engineering*.

4. Xian, H., Yang, Y., Liu, D., & Du, X. (2010). “Heat Transfer Characteristics of Oscillating Heat Pipe With Water and Ethanol as Working Fluids.” *Journal of Heat Transfer*, *132*(12), 121501.

5. Khandekar, S., & Groll, M. (2004). “An insight into thermo-hydrodynamic coupling in closed loop pulsating heat pipes.” *International Journal of Thermal Sciences*, *43*(1), 13–20.

6. Holley, B., & Faghri, A. (2005). “Analysis of pulsating heat pipe with capillary wick and varying channel diameter.” *International Journal of Heat and Mass Transfer*, *48*(13), 2635–2651.

7. Wilson, C. (2006). “Experimental Investigation of Nanofluid Oscillating Heat Pipes.” University of Missouri, 2006.

8. Hao, T., Ma, X., Lan, Z., Li, N., Zhao, Y., & Ma, H. (2014). “Effects of hydrophilic surface on heat transfer performance and oscillating motion for an oscillating heat pipe.” *International Journal of Heat and Mass Transfer*, *72*(August 2014), 50–65.

9. Zhang, F. (2015). “Wettability and Nanostructure Effect on Oscillating Heat Pipes.” (December). University of Missouri.

10. Torres, J. (2017, July). Personal communication.

11. Nam, Y., & Ju, Y. S. (2013). “A comparative study of the morphology and wetting characteristics of micro/nanostructured Cu surfaces for phase change heat transfer applications,” *Journal of Adhesion Science and Technology* 27, pp. 2163-2176.